tispin systems were typically obtained with microwave power levels of 20 mW (monoradical **2a**), 200 mW (biradical **2b**), 100 mW (triradical **2c**), or 40 mW (tetraradical **2d**), RF power levels of 200–400 W (corresponding to $B_{RF} \approx 0.6$–0.8 mT in the rotating frame), and frequency modulation amplitudes of 60–100 kHz; 100 to 200 spectra were accumulated, scan time 30 s, time constant 40 ms, 1000 data points. For comparison, the ENDOR spectrum of **1a** was recorded with an RF power of 40 W, FM amplitude of 30 kHz, and time constant 12.5 ms. NMR spectra were recorded with a Bruker AC 250 spectrometer. Mass spectra (EI) were obtained on a Varian MAT 711 double-focusing instrument.

Acknowledgment. B. K. and H. K. gratefully acknowledge financial support by the Fonds der Chemischen Industrie and the Deutsche Forschungsgemeinschaft (Normalverfahren, H. K.).

Registry No. 1, 117679-70-6; **1a**, 117679-71-7; **1b**, 117686-95-0; **1c**, 117686-96-1; **1d**, 117679-72-8; **3** (R = Me), 105309-62-4; **5**, 105309-60-2; **7**, 117679-69-3; ^{13}C, 14762-74-4; tris(4-methylphenyl)chloromethane, 117679-68-2; 4-methylphenylmagnesium bromide, 4294-57-9; tetrakis(4-bromophenyl)methane, 105309-59-9; (4-bromo-2,6-di-*tert*-butylphenoxy)trimethylsilane, 27329-74-4.

^{14}N Quadrupole Double Resonance in Some Substituted Hydroxamic Acids

Wang Ruiqin,[†] Yu Xiaolan,[†] Feng Zhenye,[†] Mian M. I. Haq,[‡] Muhammed M. P. Khurshid,[‡] Timothy J. Rayner,[‡] John A. S. Smith,*[,‡] and Michael H. Palmer[§]

Contribution from the Departments of Chemistry and Electronics, Zhongshan University, Guangzhou, China, Department of Chemistry, King's College, Strand, London WC2R 2LS, U.K., and Chemistry Department, University of Edinburgh, West Mains Road, Edinburgh EH9 3JJ, U.K. *Received April 20, 1988*

Abstract: ^{14}N quadrupole coupling constants and asymmetry parameters have been measured in a number of hydroxamic acids by double-resonance field-cycling techniques based on either irradiation in zero magnetic field or cross relaxation. The compounds all display high asymmetry parameters. Those in which this quantity is greater than 0.9 show remarkable line shapes for the two lower ^{14}N frequencies (ν_y, ν_z) in their irradiation spectra. They are explained in terms of a thermal-mixing mechanism, which generates polarization of the ^1H dipolar levels when these nearly degenerate frequencies are strongly irradiated in zero field, and then subsequently modified by level crossing when the sample is returned to high field to measure the remaining ^1H signal. Ab initio SCF–MO calculations of the ^{14}N quadrupole tensor in a group of molecules at the orientation found in crystals of acetohydroxamic acid hemihydrate and oxalodihydroxamic acid are in reasonable agreement with experiment and predict that in all the hydroxamic acids studied the maximum principal component is negative and closely parallel to the direction of the $2p_\pi$ orbital.

It has been known for many years[1] that hydroxamic acids, RCONHOH, can exist in two tautomeric forms (**1** and **2**).

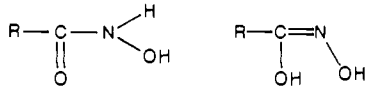

1 **2**

The equilibrium has been much studied in solution by infrared spectroscopy,[2-6] dipole moment measurements,[7-9] and ^1H, ^{13}C, and ^{17}O magnetic resonance spectroscopy,[10-14] but, apart from some infrared studies and X-ray crystal structure analyses of acetohydroxamic acid hemihydrate,[15] salicylhydroxamic acid,[16] malonohydroxamic acid,[17] nicotinohydroxamic acid,[17] and oxalodihydroxamic acid,[18] few other studies have been made of the structure of these molecules in the solid state. The purpose of this article is 3-fold: to show, first, that the two forms (**1** and **2**) can be distinguished in solids by the techniques of ^{14}N quadrupole double-resonance spectroscopy; second, that, in structure **1**, the high asymmetry parameter and short spin–lattice relaxation time in some of these compounds at room temperature lead to unusual line shapes in double-resonance irradiation experiments caused by coupling of the nearly degenerate low-frequency ^{14}N transitions ν_z, ν_y to the ^1H dipolar levels in zero magnetic field; third, that the observed quadrupole parameters can be reproduced quite closely by ab initio SCF–MO calculations and reasonably reliable directions inferred for the principal components of the ^{14}N quadrupole coupling tensor.

Experimental Section

Nine hydroxamic acids, RCONHOH, or related compounds **3–11**, were prepared for the purpose of this investigation,[19] namely, malono-

[†] Zhongshan University.
[‡] King's College.
[§] University of Edinburgh.

(1) Sidgwick, N. V. *Organic Chemistry of Nitrogen*; Taylor, T. W. J., Baker, W., Eds.; Clarendon: Oxford, 1942; Chapter VI.
(2) Mathis, F. D. *C. R. Hebd. Seances Acad. Sci.* **1951**, *232*, 505–507.
(3) Hadži, D.; Prevoršek, D. *Spectrochim. Acta* **1957**, *10*, 38–51.
(4) Horák, M.; Exner, O. *Chem. Listy* **1958**, *52*, 1451–1459.
(5) Exner, O.; Kakac, B. *Collect. Czech. Chem. Commun.* **1963**, *28*, 1656–1663.
(6) Exner, O. *Collect. Czech. Chem. Commun.* **1964**, *29*, 1337–1343.
(7) Exner, O.; Jehlička, V.; Reiser, A. *Collect. Czech. Chem. Commun.* **1959**, *24*, 3207–3221.
(8) Exner, O.; Jehlička, V. *Collect. Czech. Chem. Commun.* **1965**, *30*, 639–651.
(9) Exner, O. *Collect. Czech. Chem. Commun.* **1965**, *30*, 652–663.
(10) Mizukami, S.; Nagata, K. *Chem. Pharm. Bull.* **1966**, *14*, 1249–1255, 1263–1272.
(11) Price, B. J.; Sutherland, I. O. *Chem. Commun.* **1967**, 1070–1071.
(12) Walter, W.; Schaumann, E. *Ann. Chim. (Paris)* **1971**, *747*, 191–193.
(13) Kalinin, V. N.; Franchuk, I. F. *Zh. Prikl. Spektrosk.* **1972**, *16*, 692–698.
(14) Lipczyñska-Kochany, E.; Iwamura, H. *J. Org. Chem.* **1982**, *47*, 5277–5282.
(15) Bracher, B. H.; Small, R. W. H. *Acta Crystallogr.* **1970**, *B26*, 1705–1709.
(16) Larsen, I. K. *Acta Crystallogr.* **1978**, *B34*, 962–964.
(17) Ruiqin, W. to be published in *Jiegou Huaxue*.
(18) Lowe-Ma, C. K.; Decker, D. L. *Acta Crystallogr.* **1986**, *C42*, 1648–1649.

0002-7863/89/1511-0114$01.50/0

Table I. ^{14}N Quadrupole Resonance Frequencies (kHz), Quadrupole Coupling Constants (e^2qQ/h), and Asymmetry Parameters (η) at 291 K in Dimethylglyoxime and Some Hydroxamic Acids with $\eta < 0.9$

molecule	double resonance by irradiation in zero field					double resonance by cross relaxation				
	ν_x	ν_y	ν_z	e^2qQ/h	η	ν_x	ν_y	ν_z	e^2qQ/h	η
dimethylglyoxime (**12**)	4613	2855	1754	4979	0.706	4595	2875	1708[a]	4980	0.691
	4613	2928	1680	5027	0.670					
malonohydroxamic acid (**3**)	4610	2542	2098	4791	0.878	4650	2536	2108[b]	4791	0.882
	4645	2560	2150	4804	0.895					
salicylohydroxamic acid (**4**)			2021			4521	2601	1976[c]	4748	0.809
N-hydroxyphthalimide (**5**)						4731	2593	2164[d]	4883	0.876

[a] Two-proton flips observed at 870 and 1434 kHz. [b] Two-proton flips observed at 1262 and 2329 kHz. [c] Two-proton flips observed at 1002, 1325, and 2236 kHz. [d] Two-proton flip observed at 2312 kHz.

hydroxamic acid, $CH_2(CONHOH)_2$ (**3**), salicylohydroxamic acid, 1-$HOC_6H_4CONHOH$ (**4**), *N*-hydroxyphthalimide, $C_6H_4(CO)_2NOH$ (**5**), acetohydroxamic acid, $CH_3CONHOH$ (**6**), oxalodihydroxamic acid, $(CONHOH)_2$ (**7**), caprohydroxamic acid, $CH_3(CH_2)_4CONHOH$ (**8**), octanohydroxamic acid, $CH_3(CH_2)_6CONHOH$ (**9**), benzohydroxamic acid, $C_6H_5CONHOH$ (**10**), and nicotinohydroxamic acid, C_5H_4N-3-CONHOH (**11**).

Benzohydroxamic acid (**10**) was prepared by acylation of hydroxylamine by ethyl benzoate[19] and other hydroxamic acids (**6–9**) by appropriately modified versions of this reaction, in which the acylation reaction was performed in an alkaline solution. The hydroxylamine solution was obtained by mixing solutions of hydroxylamine hydrochloride and potassium hydroxide in methanol and filtering off the precipitated KCl. The ester was then slowly added to this solution and the mixture stirred for 5 h, the temperature being kept below 30 °C. Addition of 12 N HCl followed by distillation under reduced pressure at temperatures not exceeding 65 °C gave the hydroxamic acid as a solid residue or pastelike liquid. Acetohydroxamic acid (**6**) was extracted by boiling ethyl acetate and allowed to crystallize overnight; it was dried over silica gel and recrystallized from ethyl acetate; mp 87–88 °C (lit.[20] mp 88 °C).

Nicotinohydroxamic acid (**11**) was extracted and crystallized twice from ethanol; mp 165.5–166.5 °C (lit.[20] mp 165 °C). Caprohydroxamic acid (**8**) was extracted with water and recrystallized from the same solvent; mp 62.5–63.5 °C (lit.[20] 63.5–64.0 °C). Octanohydroxamic acid (**9**) was extracted and recrystallized twice from benzene; mp 79–79.5 °C (lit.[20] 78.5–79 °C). Malonohydroxamic acid (**3**) and oxalodihydroxamic acid (**7**) were prepared in a similar manner in alkaline methanol to obtain the sodium salt; for the former, the next step was to add water and then 6 N HCl to a pH of 5, heat to 85 °C, and then cool to obtain needlelike crystals, which were recrystallized from water: mp 165 °C (lit.[22] 165 °C). For the latter, the solution of the sodium salt was treated with 6 N HCl to a pH of 4, heated to 70 °C, and allowed to stand overnight, and the resulting crystals were recrystallized from ethanol–water; mp 154–155 °C (lit.[23] 154–155 °C). Salicylohydroxamic acid (**4**) was prepared by the action of an alkaline solution of hydroxylamine on the sodium salt of methylsalicylic acid in methanol and recrystallized twice from acetic acid; mp 167.5–168 °C (lit.[24] 168 °C). *N*-Hydroxyphthalimide was prepared by acylation in methanol and recrystallized twice from water; mp 231–232 °C (lit.[19] 232 °C). All samples were checked according to their infrared spectra and by C, H, N analyses in the case of molecules **3**, **6**, **10**, and **11**. Dimethylglyoxime was obtained from Aldrich and recrystallized from ethanol.

Because samples of only 2 g or less were available, it was necessary to use double-resonance techniques to record the ^{14}N spectra rather then conventional variable-frequency oscillators or pulsed methods, both of which require much larger amounts of material. Two double-resonance spectrometers were employed at room temperature (291 K), both of which depended on mechanical transport of the sample. One instrument has already been described;[25] the other was based on a Mid-continent Instruments pulsed radio frequency spectrometer under the control of a 6502 microprocessor.[26] Both double resonance by irradiation in zero field[27] and cross-relaxation[28] techniques were used to record spectra; in both, a field of about 16 mT was usually applied during sample transfer ("the transfer field") to reduce losses in the proton magnetization.[28] All cross-relaxation frequencies reported have been corrected for Zeeman shifts due to the presence of the magnetic field in which they are measured.[28] In most cases, the three allowed ^{14}N transitions, ν_x, ν_y, ν_z, were observed and the combinations checked from the condition that $\nu_x - \nu_y = \nu_z$.[29]

The ab initio SCF–MO calculations follow closely the methods already used in studies of the azoles,[30] cinnolinones, and other systems.[31,32] A group of molecules representing the immediate shell of neighbors to a particular NH site was computed; the basis was double-ζ (DZ) for the test molecule and either DZ or atomic orbital (minimal basis) for the adjacent molecules. The exponents and contraction coefficients were the Dunning DZ [4s2p/2s] contraction of the Huzinaga [9s4p/5s] primitive set for C, N, O, H, respectively.

Results and Discussion

All the hydroxamic acids studied gave similar quadrupole coupling constants (e^2qQ/h), around 4600–5200 kHz, with high asymmetry parameters (η) between 0.8 and 1; they are assigned structure **1**, in agreement with the evidence from infrared spectroscopy[3] and X-ray crystal structure analysis.[15–18] Their spectra however differ considerably according to whether η is smaller or larger than 0.9. Table I shows the ^{14}N frequencies for the former group of compounds, together with results for dimethylglyoxime; the spectra are straightforward to interpret, perhaps the only unusual feature being the strong two-proton relaxation jumps observed at $^1/_2\nu_x$ in cross relaxation of **3–5**. The ^{14}N quadrupole resonance spectrum of dimethylglyoxime (**12**) has already been reported,[33,34] but three groups of lines were observed in the former case[33] and one in the latter[34] whereas two would have been expected from the results of the X-ray crystal structure analysis[35] and indeed have been observed for ν_y and ν_z in the irradiation (level-crossing) spectra reported here. The molecule of malonohydroxamic acid contains two inequivalent nitrogen atoms in the crystal,[17] and separate ^{14}N spectra from them were resolved in the irradiation spectra, whereas the cross relaxation showed only a shoulder.

Table II presents results for the remaining compounds (**6–11**) in which the asymmetry parameter $\eta > 0.9$. The first five compounds in the table show very similar spectra. There are one or more lines around 5000 kHz, observed in the spectra of **13** and **7**, and a group of lines at about half this frequency observed in both irradiation and cross-relaxation spectra. Their cross-relaxation spectra have been assigned in the same way as in Table I:

(19) Blatt, A. H. *Organic Syntheses*; Wiley: New York, 1943; Collect. Vol. 2. See also: Charles, D. H.; Botteron, D. G. *J. Org. Chem.* **1946**, *11*, 207–214. Dutta, R. L. *J. Indian Chem. Soc.* **1957**, *34*, 311–316. Hurd, C. D.; Buess, C. M.; Bauer, L. *J. Org. Chem.* **1954**, *19*, 1140–1149.
(20) Inoue, Y.; Yukawa, H. *Nippon Nogei Kagaku Kaishi* **1940**, *16*, 504–509, 510–512.
(21) British Patent 1,221,393. *Chem. Abstr.* **1975**, *82*, 20210.
(22) *Beilstein, 4th ed. 2*, 555 (240).
(23) Hurd, C. D; Pilgrim, F. D. *J. Am. Chem. Soc.* **1933**, *55*, 757–759.
(24) *Merck Index*, 9th ed.; 1976.
(25) Budak, H.; Garcia, M. L. S.; Ewart, I. C.; Poplett, I. J. F.; Smith, J. A. S. *J. Magn. Reson.* **1979**, *35*, 309–318.
(26) Zhenye, F., unpublished work.
(27) Edmonds, D. T. *Phys. Rep.* **1977**, *29C*, 233–290.
(28) Stephenson, D.; Smith, J. A. S. *Proc. R. Soc. London, A* **1988**, *416*, 149–178.
(29) Smith, J. A. S. *Chem. Soc. Rev.* **1986**, *15*, 225–260.
(30) Palmer, M. H.; Stephenson, D.; Smith, J. A. S. *Chem. Phys.* **1985**, *97*, 103–111.
(31) Palmer, M. H.; Gould, R. O.; Blake, A. J.; Smith, J. A. S.; Stephenson, D.; Ames, D. *Chem. Phys.* **1987**, *112*, 213–225.
(32) Palmer, M. H.; Haq, M. M. I.; Stephenson, D.; Smith, J. A. S. *Chem. Phys. Lett.* **1986**, *127*, 615–619.
(33) Sauer, E. G.; Bray, P. J. *J. Chem. Phys.* **1973**, *58*, 21–26.
(34) Hsieh, Y.-N.; Ireland, P. S.; Brown, T. L. *J. Magn. Reson.* **1976**, *21*, 445–456.
(35) Merritt, L. L., Jr.; Lauterman, E. *Acta Crystallogr.* **1952**, *5*, 811–817.

Table II. ^{14}N Quadrupole Resonance Frequencies (kHz), Quadrupole Coupling Constants (e^2qQ/h), and Asymmetry Parameters (η) at 291 K in Some Hydroxamic Acids with $\eta > 0.9$

molecule	zero-field irradiation				cross relaxation			
	ν_z, ν_y	ν_x	e^2qQ/h	η	ν_z, ν_y	ν_x	e^2qQ/h	η
acetohydroxamic acid (**6**)	2159	4652	4797	0.915	2208[a]	4719[b]	4838	0.913
	2230				2366			
	2460				2524			
	2539							
acetohydroxamic acid hemihydrate (**13**)	2339	4845	4833	0.981		4837[b]		
	2402							
	2471							
oxalodihydroxamic acid (**7**)	2372	5114	5133	0.938	2435[c]		5158	0.944
	2452				2535			
	2613				2651			
	2679							
caprohydroxamic acid (**8**)	2396		5128	0.945	2443[d]		5146	0.949
	2452				2535			
	2592				2638			
	2664							
octanohydroxamic acid (**9**)	2376		5126	0.942	2418[e]		5135	0.942
	2455				2535			
	2594				2642			
	2679							
benzohydroxamic acid (**10**)	2489				2570[f]		5298	0.970
	2597				2630			
					2686			
nicotinohydroxamic acid (**11**)[g]	2404		4808	1	2397	4832	4794	1

[a] Two-proton relaxation jumps were detected at 1117 and 1259 kHz. [b] Detected as a step only, due to level-crossing effects.[28] [c] Two-proton relaxation jumps were detected at 1212 and 1320 kHz. [d] Two-proton relaxation jumps were detected at 1200 and 1326 kHz. [e] Two-proton relaxation jumps were detected at 1219 and 1327 kHz. [f] Two-proton relaxation jumps were detected at 1302 and 1348 kHz. [g] ^{14}N pyridine signals were seen at 559, 2578, and 3134 kHz in cross relaxation and 592 and 3201 kHz in irradiation spectra, giving e^2qQ/h = 3808 kHz and $\eta = 0.29_4$.

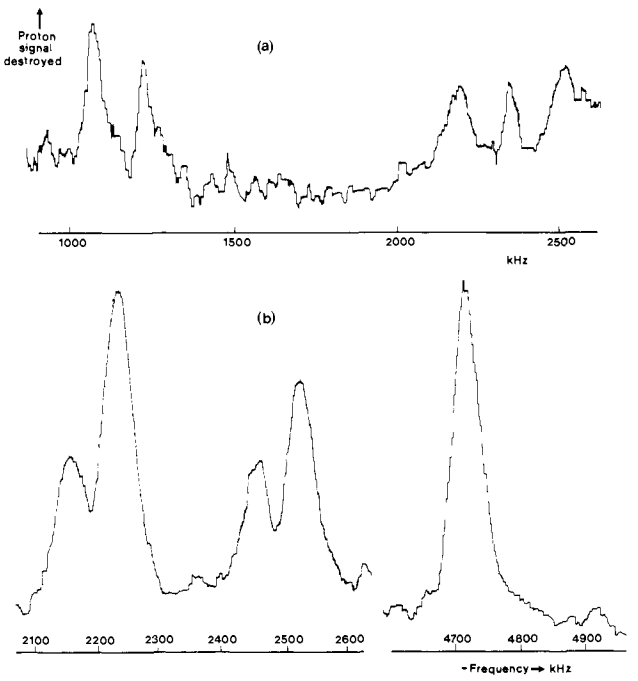

Figure 1. ^{14}N quadrupole double-resonance spectra of recrystallized $CH_3CONHOH$ at 291 K (a) by cross relaxation (τ_P = 15 s, τ_{CR} = 2 s) and (b) by irradiation in zero field (τ_P = 11 s, τ_Q = 2 s); rf 300 V (both by diode detection).

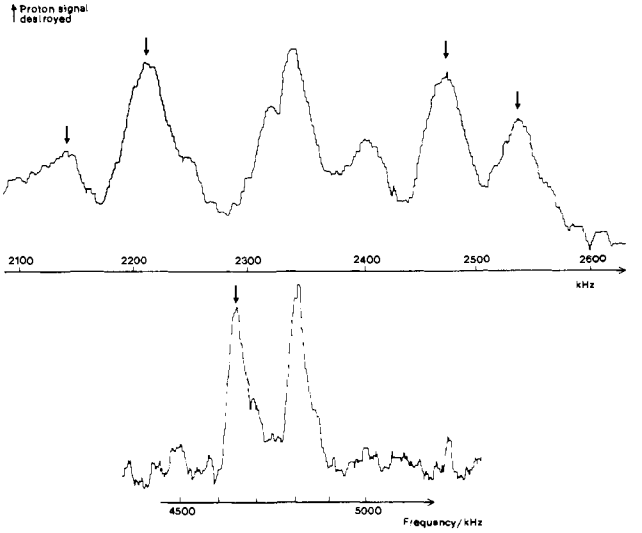

Figure 2. ^{14}N quadrupole double-resonance spectra at 291 K of a mixture of acetohydroxamic acid and its hemihydrate; lines assigned to the former are marked by arrows. The spectra were obtained by irradiation in zero field and diode detection of the high-field ^1H signal.

the lower and higher frequency peaks in the triplet near 2300–2600 kHz were assigned to ν_z and ν_y, respectively, giving the quadrupole coupling constants and asymmetry parameters shown in the last two columns of Table II. This assignment leaves unresolved the problem of the origin of the high-frequency lines in the irradiation and cross-relaxation spectra and the multiplets observed in the irradiation spectra around 2400 kHz. Except for benzohydroxamic acid (**10**) and nicotinohydroxamic acid (**11**) (in which the spectra are overlapped by pyridine ^{14}N signals), the general pattern is for the zero-field irradiation spectra to show a low-frequency "quadruplet" and the cross-relaxation spectra a low-frequency doublet already assigned to ν_z, ν_y, with a sharp central peak midway between. The high-frequency lines are usually singlets in irradiation and steplike in cross relaxation. Figure 1 shows the spectra for acetohydroxamic acid crystallized from dry ethyl acetate. The most obvious explanation of this behavior would be crystallographic nonequivalence, but it is then difficult to believe that *all* molecules **6**–**11** have the same number of nitrogen atoms in the asymmetric unit of the structure. Dipolar interaction of the ^{14}N nucleus with the attached hydrogen atom is also unlikely to account for the splitting; at an N–H distance of 1.05 Å, the $^{14}N\cdots{}^1H$ dipole–dipole coupling constant $h\gamma_H\gamma_N/2\pi r_{NH}^3$ is only 7.5 kHz, but the first-order interaction is quenched for $\eta > 0$[36,37] and only the much smaller second-order effect should be observed.

(36) Leppelmeier, G. W.; Hahn, E. L. *Phys. Rev.* **1966**, *141*, 724–731.
(37) McEnnan, M. M.; Scott, T. A. *Am. J. Phys.* **1972**, *40*, 1158–1166.

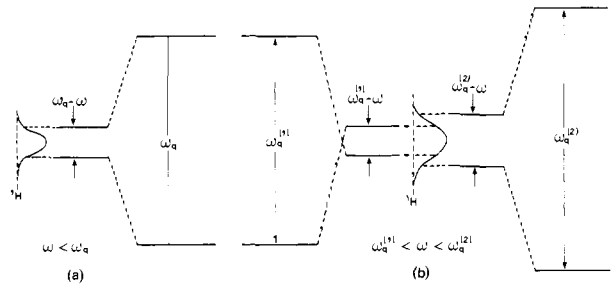

Figure 3. Energy levels in a frame rotating at an angular frequency of ω for (a) one quadrupole resonance frequency ω_Q and (b) a pair of close frequencies $\omega_Q^{(1)}$ and $\omega_Q^{(2)}$.

Acetohydroxamic acid presents other problems. Samples purchased from Aldrich show poorly reproducible spectra, with two lines in the high-frequency region and a complex multiplet between 2100 and 2600 kHz (Figure 2); they analyze as variable mixtures of the anhydrous material and the hemihydrate, the crystal structure of which is known to contain only one molecule in the asymmetric unit.[15] Some of the lines in this complex spectrum, marked by arrows in Figure 2, are found in the spectrum shown in Figure 1, to which this sample reverts on crystallization from dry ethyl acetate. The spectra in Figure 2 are therefore assumed to arise from a mixture of the anhydrous material and the hemihydrate, and the frequencies listed for the latter in Table II have been obtained in this way. Once again, the X-ray point symmetry[15] would have predicted only a pair of ν_z, ν_y lines, whereas three are actually observed in this region. Note that an additional peak in Figure 2 at 2323 kHz is close to half of the frequency of ν_x and may therefore arise from first-harmonic excitation.

The spectral evidence indicates that the high-frequency lines in the spectra of acetohydroxamic and oxalodihydroxamic acid belong to ν_x and are observed by level-crossing; since their cross-relaxation spectra are weak, the ^{14}N spin–lattice relaxation times (T_{1Q}) must be long[27] and the ^1H spin–lattice relaxation time in zero field (T_{1D}) not too short. This conclusion is supported by the steplike appearance of the ν_x signal in acetohydroxamic acid and the hemihydrate, a line shape that arises when T_{1Q} is longer than the ^1H spin–lattice relaxation time in low field and is due to level-crossing effects.[28] In contrast, the low-frequency lines, ν_y, ν_z, give reasonable cross-relaxation spectra, suggesting that their ^{14}N spin–lattice relaxation times are comparable to or shorter than the ^1H spin–lattice relaxation times in the cross-relaxation field. It might be possible to observe level-crossing spectra under such conditions, particularly if the transit time into high field was short and a transfer field was used, but a doublet structure would not be expected. Such lines shapes are typical of thermal-mixing spectra[38] and are common in double-resonance spectroscopy of half-integral spin quadrupolar nuclei.[39] They arise as a result of direct thermal contact between the ^1H dipolar levels and a pair of quadrupole levels when the latter are irradiated in zero magnetic field. In a frame rotating at the irradiation (angular) frequency ω (Figure 3a), the "effective" frequency seen by the nucleus in a sufficiently large radio frequency field H_{1Q} is $\Delta\omega = \omega_Q - \omega$, where ω_Q is the quadrupole resonance frequency. If $\Delta\omega$ lies within the ^1H dipolar absorption edge, energy transfers to or from the protons can occur, driven by the radio frequency field. They are zero when $\Delta\omega = 0$, which accounts for the dip at the line center. Off resonance, the thermal-mixing line shape is given by[40] eq 1 in which

$$\frac{\beta^P}{\beta^P_L} = \frac{WT_{1D}\omega_Q(\Delta\omega/D^2)}{1 + WT_{1Q} + WT_{1D}(\Delta\omega/D)^2} \quad (1)$$

β^P ($=\hbar/kT$) is the ^1H inverse spin temperature (β^P_L being its equilibrium value), D is the local frequency equal to $\gamma H'_L$, where H'_L is the local field,[41] and W is the Q-spin transition probability (eq 2), $g(\Delta\omega)$ being the Q line-shape function. According to eq

$$W = \pi\gamma_Q H_{1Q}^2 g(\Delta\omega) \quad (2)$$

1, a true thermal-mixing line-shape function changes sign at the line center corresponding to cooling of the ^1H dipolar levels when $\omega < \omega_Q$ (Figure 3a) and to heating when $\omega > \omega_Q$; rapid transfer of the sample to high field transforms dipolar into Zeeman order, and the observed ^1H magnetic resonance signal should follow the same equation.

The theory needs some modification to allow for the fact that two close quadrupole resonance transitions of the same ^{14}N nucleus, namely ν_z and ν_y when $\eta \Rightarrow 1$, may both be driven by the radiation. The appropriate theory to use is then thermal mixing in a frame rotating at different frequencies with respect to two close transitions of the same spin species, say $\omega_Q^{(1)}$ and $\omega_Q^{(2)}$ (Figure 3b).[38] The rates of change of the level populations, as expressed in terms of the quadrupolar inverse spin temperatures α_1 and α_2, are given by the Provotorov equations (eq 3). These

$$\frac{d\alpha_1}{dt} = -W_Q^{(1)}(\alpha_1 - \beta^P) - \frac{1}{T_{1Q}^{(1)}}(\alpha_1 - \alpha_L^{(1)}) \text{ (for } \omega_Q^{(1)}) \quad (3)$$

$$\frac{d\alpha_2}{dt} = -W_Q^{(2)}(\alpha_2 - \beta^P) - \frac{1}{T_{1Q}^{(2)}}(\alpha_2 - \alpha_L^{(2)}) \text{ (for } \omega_Q^{(2)})$$

$$\frac{d\beta^P}{dt} = W_Q^{(1)}\frac{\Delta\omega_1^2}{D^2}(\alpha_1 - \beta^P) + W_Q^{(2)}\frac{\Delta\omega_2^2}{D^2}(\alpha_2 - \beta^P) - \frac{1}{T_{1D}}(\beta^P - \beta^P_L)$$

can be solved under steady-state conditions

$$\frac{d\alpha_1}{dt} = \frac{d\alpha_2}{dt} = \frac{d\beta^P}{dt} = 0 \quad (4)$$

to yield

$$\frac{\beta^P}{\beta^P_L} = \left[1 + T_{1D}\left\{\omega_Q^{(1)}\frac{\Delta\omega_1}{D^2}\left(\frac{W_Q^{(1)}}{1 + W_Q^{(1)}T_{1Q}^{(1)}}\right) + \omega_Q^{(2)}\frac{\Delta\omega_2}{D^2}\left(\frac{W_Q^{(2)}}{1 + W_Q^{(2)}T_{1Q}^{(2)}}\right)\right\}\right] \Bigg/ \left[1 + T_{1D}\left\{\left(\frac{\Delta\omega_1}{D}\right)^2\left(\frac{W_Q^{(1)}}{1 + W_Q^{(1)}T_{1Q}^{(1)}}\right) + \left(\frac{\Delta\omega_2}{D}\right)^2\left(\frac{W_Q^{(2)}}{1 + W_Q^{(2)}T_{1Q}^{(2)}}\right)\right\}\right] \quad (5)$$

making the usual assumptions that

$$\alpha_L^{(1)} = \beta^P_L\frac{\omega_Q^{(1)}}{\Delta\omega_1} \qquad \alpha_L^{(2)} = \beta^P_L\frac{\omega_Q^{(2)}}{\Delta\omega_2} \quad (6)$$

Near to either one of the two quadrupole resonance frequencies, say $\omega_Q^{(1)}$, the other transition probability may be set equal to zero, and if we are off saturation, $W_Q^{(1)}T_{1Q}^{(1)}$, $W_Q^{(2)}T_{1Q}^{(2)} < 1$ and eq 5 reduces to eq 1, giving a typical thermal-mixing line shape centered on $\omega_Q^{(1)}$. The same argument applies near $\omega_Q^{(2)}$. In the intermediate region, $\Delta\omega_1$ and $\Delta\omega_2$ in the numerator of eq 5 are comparable but have opposite signs; as Figure 3b illustrates, the net transfers to the ^1H dipolar system are therefore a balance of two terms of opposite sign. The ^1H dipolar inverse spin temperature is again zero or very small when

$$\omega_Q^{(1)}\Delta\omega_1 W_Q^{(1)} + \omega_Q^{(2)}\Delta\omega_2 W_Q^{(2)} = 0 \quad (7)$$

i.e. close to $\Delta\omega_1 = -\Delta\omega_2$. The efficiency of energy transfers to and from the ^1H dipolar bath in this region appears to be largely responsible for the observation of thermal-mixing line shapes, a

(38) Goldman, M. *Spin Temperature and Nuclear Magnetic Resonance in Solids*; Clarendon: Oxford, 1970.
(39) Stephenson, D.; Smith, J. A. S. *J. Mol. Struct.* **1983**, *111*, 43–52.
(40) Poplett, I. J. F.; Smith, J. A. S. *J. Chem. Soc., Faraday Trans. 2* **1981**, *77*, 1155–1173.
(41) Abragam, A.; Proctor, W. G. *Phys. Rev.* **1958**, *109*, 1441–1458.

rare feature in ^{14}N quadrupole double-resonance spectroscopy.

The ^1H signal observed in high field as the irradiation frequency ω in zero field is varied should therefore follow eq 5, but it is clear from the spectra in Figures 1 and 2 that it does not do so. Distortions of the ideal thermal-mixing line shape may be observed when diode detection is used (as in Figures 1 and 2) and T_{1D} is short,[39] but the true line shape should be observed if phase-sensitive detection is used, which again is not the case in these experiments: diode and phase-sensitive detection give similar doublet spectra, differing only in the greater intensity difference in the latter.

However, the observed line shapes are consistent with the operation of *both* thermal-mixing and level-crossing mechanisms. In zero field, thermal mixing generates ^1H dipolar polarization, except when $\Delta\omega_1 = \Delta\omega_2 = 0$ or $\Delta\omega_1 = -\Delta\omega_2$, which then undergoes level crossing with the ^{14}N levels when the sample is returned to high field. Since the ^{14}N levels have been heated by irradiation in zero field, the level-crossing transfers will always be in such a direction as to heat the ^1H levels, so the cooling created in zero field when $\omega < \omega_Q$ is destroyed and even inverted and the heating created when $\omega > \omega_Q$ is enhanced (Figure 3b). The result is an asymmetrical-looking curve corresponding to ^1H polarization destroyed on either side of the minimum but less so when $\omega < \omega_Q$, when thermal-mixing and level-crossing effects have the opposite sign, to when $\omega_Q < \omega$, when they have the same sign.

These conclusions may be expressed in quantitative terms by use of the level-crossing equations for the ^1H population p' at the end (high field) of a level-crossing cycle[27]

$$p' = \left(\frac{3}{4}X^3 - \frac{1}{4}X^2 + \frac{1}{2}X\right)p_{TM} + \frac{1}{2}(1 - X)\left\{\left(-\frac{3}{4}X^2 - 1\right)a + \left(\frac{3}{4}X^2 - \frac{1}{2}x\right)b + \left(\frac{1}{2}X + 1\right)c\right\}$$

in which p_{TM} is the thermal-mixing population created by irradiation in zero field, the ^1H populations being written as $P(1 + p)$ and ^{14}N as $Q(1 + c)$, $Q(1 + b)$, $Q(1 + a)$ and $X = P/P + Q$ where $N_P = 2P$ and $N_Q = 3Q$, N_P and N_Q being the numbers of protons and nitrogen nuclei in the molecule. The thermal-mixing population is related to the ^1H inverse spin temperature by the expression

$$p = \frac{1}{2}\gamma H\beta^P \tag{8}$$

For acetohydroxamic acid, $X = 0.882$ and eq 8 becomes

$$p' = 0.761p_{TM} - 0.0935a_0 + 0.00844b_0 + 0.0850c_0 \tag{9}$$

in which a_0, b_0, and c_0 refer to the ^{14}N populations in zero field. The argument is that although p_{TM} (from eq 1) changes sign at the line center, the remaining terms on the right-hand side of eq 9 ensure that p', the recovered ^1H population in high field, always has the same sign. To put this in quantitative terms unfortunately requires a knowledge of the ^1H and ^{14}N relaxation times; an estimate can however be obtained if all relaxation times are assumed to be short compared to the cycle time. Populations are written in frequency units, i.e. in units of h/kT or kilohertz for convenience, and are calculated at three positions in the line shape of Figure 1b, namely off resonance, at the minimum at the line center and at the two maxima (it should be recalled that the vertical axis in this figure represents decreasing recovered ^1H signal). Off resonance from ν_z, we may take $-a = c$ and $b = 0$ for a nearly equispaced three-level system and with $c = 2300$ kHz and $p_{TM} = 0$ obtain a recovered ^1H signal of 410 kHz, still a loss compared to that in the absence of double resonance. At the line center with ν_z saturated, we may take $a = b = {}^1/_2c$ and with p_{TM} still zero obtain a recovered ^1H signal of 196 kHz. At the line maxima, differentiation of eq 1 yields[38]

$$\frac{\beta^P{}_{max}}{\beta^P{}_L} = \frac{\omega_Q}{2D}\left(\frac{T_{1D}}{T_{1Q}}\right)^{1/2} = \frac{\omega_Q}{2\Delta\omega_{max}} \tag{10}$$

which for ν_z in Figure 1b equals 30.7. It is only possible to guess $\beta^P{}_L$ and, in any case, the ^1H signal recovered is reduced by spin–lattice relaxation during the return half of the cycle. If we take a value of 0.5 kHz and assume $c = {}^1/_2$, $b = {}^1/_5$, and $a = {}^{-3}/_{10}$, the recovered ^1H signal becomes 158 ± 15, the upper sign referring to the low-frequency maximum and the lower to the high-frequency maximum. The sequence of calculated values is in rough consistency with the line shape of Figure 1b. The spectra of the last two compounds in Table II show other features. In the case of nicotinohydroxamic acid, only one frequency could ever be resolved in the region of 2400 kHz, heavily overlapped by ν_y of the pyridine nitrogen, so it appears that η is almost exactly unity in this compound. In benzohydroxamic acid, a doublet was observed in irradiation, the lower frequency component at 2489 kHz being the stronger; the cross-relaxation spectra revealed however a poorly resolved triplet, although the two-proton jump was clearly a doublet. In this case, it seems that only ν_z is observed in the irradiation spectra, which have a long high-frequency tail due possibly to ν_y. This transition is also the weaker of the two in all the other compounds in Table II in which it is resolved.

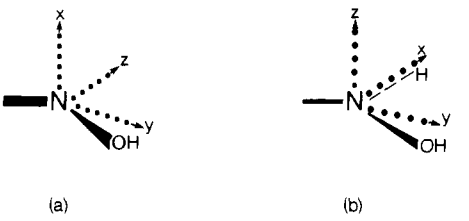

Figure 4. Possible orientations of the ^{14}N electric field gradient axes in (a) oximes and (b) hydroxamic acids.

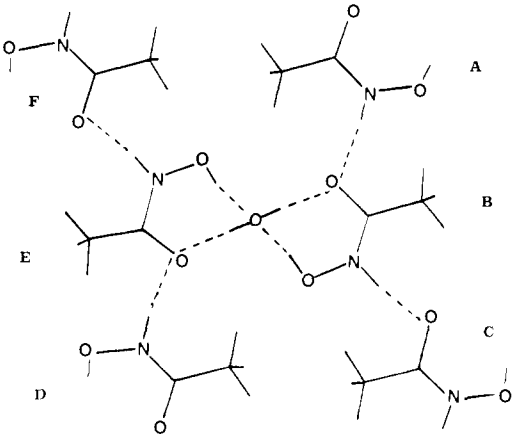

Figure 5. Diagram of the immediate environment of acetohydroxamic acid and water in crystals of the hemihydrate.

In conclusion, we discuss the magnitudes and most likely orientations of the ^{14}N quadrupole tensors in oximes and hydroxamic acids and their relationship to electronic structure. In both cases the high asymmetry parameters make it difficult to be sure of the correct orientation of q_{yy} and q_{zz}. In oximes, the orientation shown in Figure 4a has been proposed for monoalkyl-substituted aldoximes[33,42] with e^2qQ/h negative; the quadrupole coupling constant in these compounds is almost unchanged in magnitude (4900 ± 300 kHz) over a wide range of η (0.4–0.9), suggesting that the major changes are occurring in the magnitudes of q_{xx} and q_{yy} without change in orientation and therefore that electronic charge is being redistributed in the x–y plane as the substituents are changed. This in turn implies that the N $2p_\sigma$ orbital lies close to the z axis with a constant population (close to 2) and that substituents vary the degree of polarization of the C=N bond through the π system via RCH=N—X ↔ RCH—N^+—X^-, as Sauer and Bray have proposed.[33] In contrast, in the hydroxamic acids both quadrupole coupling constant and asymmetry parameter vary together so that it is necessary to turn to more precise calculations of the ^{14}N quadrupole tensor. These

(42) Palmer, M. H. *Z. Naturforsch., A: Phys., Phys. Chem., Kosmophys.* **1986**, *41A*, 147–162.

Table III. Total Energies (au)[a] for Each Molecule/System Studied and the Total Basis Functions Used

calculation	basis set	energy, au
A. Acetohydroxamic Acid		
1. monomer, NH = 0.90 Å	60	−282.514 23
2. monomer, NH = 0.973	60	−282.522 40
3. monomer, NH = 1.013	60	−282.523 01
4. trimer + $2H_2O$, NH = 0.90 Å (see text)	208	−999.568 61
B. Oxalodihydroxamic Acid		
1. monomer, NH = 0.84 Å	88	−486.053 30
2. monomer, NH = 0.951 Å	88	−486.119 15
3. monomer, NH = 1.02 Å	88	−486.124 85
trimer molecules A–C	176	−1455.41 301
trimer molecules A, B, and D	176	−1455.41 203

[a] 1 au = 2626 kJ mol^{-1}.

Table IV. Mulliken Analyses for Monomeric and Central Test Molecules of the Molecular Groups

	NH	CO	CH_3	OH
A. Acetohydroxamic Acid				
(a) monomer	8.0497	14.0838	8.8394	9.0272
(b) hemihydrate group[a]	8.0100	14.1993	8.7752	9.0302
B. Oxalodihydroxamic Acid				
(a) monomer	7.9609	14.0048		9.0343
(b) trimer A–C	7.9314	14.0424		9.0469
(c) trimer A, B, and E	7.9210[b]	14.0298[b]		9.0376[b]
	7.9484[c]	14.0054[c]		9.0283[c]

[a] Small variations from 40.00*e* in total arise from the small group of molecules with a *net* acceptance from neighbors, in contrast to the neutral real lattice. [b,c] Represent the fully H bonded and free sides of the unsymmetrically H-bonded system, respectively.

have been performed for both acetohydroxamic acid hemihydrate (Figure 5) and oxalodihydroxamic acid (Figure 6) for groups of molecules at orientations taken from their X-ray crystal structure analysis.[15,18] It should be noted that the determined N–H lengths are significantly smaller (0.90 and 0.84 Å, respectively) than expected (ca. 1.00 Å) and that this arises from deficiencies in the X-ray analysis. In the case of the single molecule calculations, we investigated other N–H lengths (all other coordinates being constant), and this led to values closer to expectation. The electric field gradients (proportional to the ^{14}N nuclear quadrupole coupling constant) were evaluated at each geometry.

In solid acetohydroxamic acid hemihydrate, the organic moieties A–C (Figure 5) lie in a stepped sequence at $z = {}^1/_2, 0, -{}^1/_2$, and by rotation about a 2-fold axis, passing through the H_2O molecule lead to molecules D–F (space group *Pnn*2).[15] A test molecule (B) is H-bonded to NH(A) as a donor and to CO(C) as an acceptor; there are additional H bonds to *two* H_2O molecules through CO(B)···H and OH(B)···O, so that notwithstanding the hemihydrate stoichiometry, the immediate environment of one test molecule (B) is A + B + C + $2H_2O$. This unit was computed in a DZ basis (208 functions). In the case of oxalodihydroxamic acid,[18] the H bonding is more complex, owing to the extra polar groups. The units around one molecule (A, Figure 2) in the space

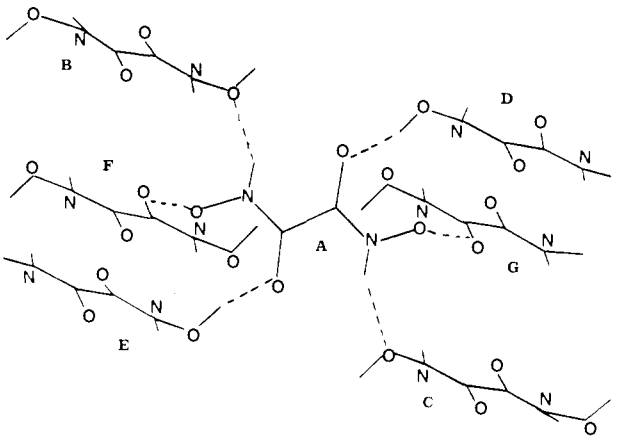

Figure 6. Diagrammatic representation of part of the crystal structure of oxalodihydroxamic acid.

group $P2_1/n$ show H-bonding NH(A)···OH(B, C), CO(A)···HO(D, E), and OH(A)···OC(F, G). Thus, a full nearest-neighbor environment would contain A, B, ···, G, which is beyond the current capacity of our computing facilities. A much smaller system was hence sought; since the major contributions to the ^{14}N quadrupole components are likely to arise from (a) the immediate neighbor *atoms* and (b) factors such as amide resonance, it was felt that the effects of molecules F, G, by H bonding to H(O) would be very small at N(A) and were therefore neglected. It seemed necessary to assess the effects of both the NH (A) and CO(A) H bonding, and this was achieved by two smaller calculations on trimeric units A, B, C and A, B, E, each of 176 functions; the former treats the test molecules symmetrically while the latter has a more complete environment on one side of the dihydroxamic acid system, with the other half as in the free molecule. As with the acetohydroxamic acid case, calculations were also performed on the free molecule A, with three different N–H bond lengths. However, these calculations for each monomeric system showed (Table III) that the energy minima for these single-variable studies lie near N–H = 1.02 Å, and the variations produced little change in other properties such as atomic populations of the constituent groups (Table IV) or electric field gradient (Table V). Thus, we proceeded with N–H = 1.020 Å in the main calculations.

The results of these calculations of the magnitudes and directions of the ^{14}N quadrupole coupling components in both systems are summarized in Table V. The computed electric field gradients (q_{ii}, EFG) have been converted to the corresponding ^{14}N nuclear quadrupole coupling components (X_{ii}, NQCC) by the relationship

$$X_{ii} = Q_N q_{ii} \tag{11}$$

The value for the ^{14}N electric quadrupole moment Q_N was taken as 1.72 fm^2; this value is lower than recent experimental[43] and

Table V. Computed ^{14}N Quadrupole Coupling Components (X_{ii}, MHz) and Electric Field Gradients (q_{ii}, au) Compared with the Experimental Values at 291 K

	X_{xx} (q_{xx})	X_{yy} (q_{yy})	X_{zz} (q_{zz})	η
A. Acetohydroxamic Acid Hemihydrate				
	0.5540 (−0.1572)	4.3629 (−1.2379)	−4.9169 (+1.3951)	0.775
expt, MHz	0.046	4.787	(−)4.833	0.981
B. Oxalodihydroxamic Acid				
A, B, and E	0.5452 (−0.1547)	4.3456 (−1.2330)	−4.8908 (+1.3877)	0.777
A–C	0.6019 (−0.1708)	4.4690 (−1.2680)	−5.0710 (+1.4388)	0.763
expt, MHz	0.159	4.974	(−)5.133	0.938
C. Acetohydroxamic Acid				
monomer	1.2757 (−0.3618)	4.3072 (−1.2221)	−5.5829 (+1.5839)	0.543
D. Oxalodihydroxamic Acid				
monomer	1.0090 (−0.2863)	4.2391 (−1.2028)	−5.2482 (+1.4891)	0.615

Table VI. Calculated Principal ^{14}N Quadrupole Coupling Components (MHz) for the Acetohydroxamic Acid Molecule

N–H, Å	X_{zz}	X_{yy}	X_{xx}	η
0.90	−5.4970	4.3876	1.1095	0.596
0.97	−5.5413	4.3382	1.2031	0.566
1.013	−5.5823	4.3072	1.2751	0.543

theoretical[44] values but is here regarded as a scaling parameter, based upon least-squares fitting of X_{ii} with calculated q_{ii} *using the same basis set*.[45] The value will clearly be basis set dependent.

For both molecules the direction of X_{zz} lies in the local π direction, i.e. perpendicular to the C–N–H plane (Figure 4b). However, the asymmetry parameter is very high, so that X_{yy} is close in magnitude (but opposite in sign); the direction of X_{yy} is predicted to lie relatively close to the N–O bond so that the direction of the smallest component X_{xx} lies in the C–N–O–H plane at an angle of about 30° to the N–H bond rotated toward N–O. Thus, despite the similarity of quadrupole coupling constant and asymmetry parameter to the oximes, the two differ by an interchange in the directions of the components q_{xx} and q_{zz}.

Although there are small changes in direction between the monomers and the H-bonded calculated values, these are not significant; the variation with N–H distance is also small, as is shown in Table VI for the monomeric acetohydroxamic acid molecule.

As N–H increases, the magnitudes of both X_{zz} and X_{xx} are predicted to increase (but with opposite sign); there is a rather smaller change in X_{yy}, so that the effect in η is a decline with increasing N–H length. The changes are however sufficiently small that we can be reasonably confident of the assignment of the calculated data and the axial systems to the experimental magnitudes (Table V and Figure 4b).

It is worth noting that the individual total atomic populations of the NH groups also vary with the N–H length, although the sum is effectively constant; thus, for N–H = 0.84, 0.95, and 1.02 Å in oxalodihydroxamic acid, the N/H populations are 7.125/0.829, 7.234/0.714, and 7.302/0.659, respectively.

Comparison of the single molecule calculations with the H-bonded species shows that η increases in the latter and that this arises from a fall in magnitude of X_{zz} (and X_{xx}), with X_{yy} little changed. These changes are in sign and magnitude very similar to those which occur for N(1)H in the imidazole molecule on passing from the gas to the solid state,[30] and their origin in both molecules seem to lie in a loss of about 0.05–0.08*e* of charge from $2p_\pi$ and a similar increase in $2p_\sigma$ at N–H when hydrogen bonding occurs. Significant changes also occur in the –CO–NH system of the hydroxamic acid molecule, some of the N $2p_\pi$ charge density finding its way into the (C)O $2p_\pi$ orbital. The single molecule calculations on acetohydroxamic acid (Table IV) also show that the individual groups CO, NH, and OH are all net recipients of charge (in decreasing amounts) from the CH_3 group (which is about 0.16*e* deficient). Hydrogen is a donor to all C, N, O atoms as expected.

When the acetohydroxamic acid is complexed to its neighbors, including the H_2O molecules, the carbonyl oxygen atom is a major recipient (0.1*e*) largely at the expense of the CH_3 and (less) NH groups. Overall, the organic molecule remains nearly neutral as expected.

The absence of a donor CH_3 group in oxalodihydroxamic acid leads to the NH group being a net donor to its neighboring groups CO and OH, and as a consequence it is the N rather than the H atom that is principally affected.

In conclusion, we need to assess the reliability of the assignment of the ^{14}N quadrupole components made in Table V and Figure 4b. Both calculation and experiment lead to large values of $|X_{zz}|$ and $|X_{yy}|$, with very small X_{xx} and hence high η. The calculated η lies below that observed in either molecular system, and we cannot therefore be absolutely certain that X_{zz}(calc) relates to the same axis as X_{zz}(obs). Evidence in support of the direct identity of these two can be obtained by comparison with related molecules. Hydroxamic acids are special cases of amides, for which it has long been assumed,[46] and confirmed by recent ab initio studies, that X_{zz} can be identified with X_π. This has been confirmed experimentally in several cases; some examples from microwave spectroscopy are formamide[47] and urea.[48] In our experience of using ab initio SCF–MO calculations,[30,31,42,49,50] all amides so far studied have the identity $X_{zz} = X_\pi$. However, hydroxamic acids have other analogies relating to the presence of a N–O bond; thus, hydroxylamine,[51] isoxazole,[52] nitrosomethane,[53] and formaldoxime[42] all have high *positive* X_{ii} closely parallel to the N–O bonds.[42] These molecules may be regarded as having essentially a $2p_\sigma$ lone pair of electrons on N, resulting in high *negative* X_{ii} close to that axis. Thus, in all these cases we have $\eta \approx 0.9$. The same is true for the oximes; the large negative value of X_{ii} lies roughly parallel to a $2p_\sigma$ N orbital, the large positive value again lies along the N–O bond, and so the *x* and *z* directions interchange with respect to the hydroxamic acids.

Acknowledgment. We thank the SERC for equipment grants and a research assistantship (T.J.R.), the Pakistan Government for Scholarships to M.M.I.H. and M.M.P.K., and the British Council, Great Britain–China Educational Trust, and Henry Lester Trust for grants (F.Z.).

Registry No. 3, 1882-99-1; **4**, 89-73-6; **5**, 524-38-9; **6**, 546-88-3; **7**, 1687-60-1; **8**, 4312-93-0; **9**, 7377-03-9; **10**, 495-18-1; **11**, 5657-61-4; **12**, 95-45-4.

(43) Winter, H.; Andrä, H. J. *Phys. Rev. A* **1980**, *A21*, 581–587.
(44) Sundholm, D.; Pyykkö, P.; Laaksonen, L.; Sadlej, A. J. *Chem. Phys.* **1986**, *101*, 219–225.
(45) Redshaw, M.; Palmer, M. H.; Findlay, R. H. *Z. Naturforsch., A: Phys., Phys. Chem., Kosmophys.* **1979**, *34A*, 220–232. Palmer, M. H.; Simpson, I.; Findlay, R. H. *Z. Naturforsch., A: Phys., Phys. Chem., Kosmophys.* **1981**, *36A*, 34–50.
(46) Lucken, E. A. C. *Nuclear Quadrupole Coupling Constants*; Academic: London, 1969; p 224.
(47) Costain, C. C.; Dowling, J. M. *J. Chem. Phys.* **1960**, *32*, 158–165.
(48) Brown, R. D.; Godfrey, P. D.; Storey, J. *J. Mol. Spectrosc.* **1975**, *58*, 445–450.
(49) Rabbani, S. R.; Edmonds, D. T.; Gosling, P.; Palmer, M. H. *J. Magn. Reson.* **1987**, *72*, 230–237.
(50) Palmer, M. H.; Blake, A. J.; Gould, R. O. *Chem. Phys.* **1987**, *115*, 219–227.
(51) Tasunekawa, S. *J. Phys. Soc. Jpn.* **1972**, *33*, 167–174.
(52) Stiefvater, O. L.; Nösberger, P.; Sheridan, J. *J. Chem. Phys.* **1975**, *9*, 435–444. Stiefvater, O. L. *J. Chem. Phys.* **1975**, *63*, 2560–2569. Lowe, S. E.; Sheridan, J. *Chem. Phys. Lett.* **1978**, *58*, 79–82.
(53) Coffey, D., Jr.; Britt, C. O.; Boggs, J. E. *J. Chem. Phys.* **1968**, *49*, 591–600.